Thin Solid Films 636 (2017) 658–663

Contents lists available at ScienceDirect

Thin Solid Films

journal homepage: www.elsevier.com/locate/tsf

Structural and compositional characterization of single crystal uranium dioxide thin films deposited on different substrates

Mohamed S. Elbakhshwan *, Brent J. Heuser

Department of Nuclear, Plasma, and Radiological Engineering, University of Illinois Urbana Champaign, USA

ARTICLE INFO

Article history:
Received 18 October 2016
Received in revised form 7 July 2017
Accepted 8 July 2017
Available online 10 July 2017

Keywords:
Uranium dioxide
Magnetron sputtering
Thin film
Single crystal
X-ray diffraction
Different substrates
Peak splitting

ABSTRACT

Uranium dioxide thin films were deposited on single crystal TiO_2, Al_2O_3, YSZ, ZnO and $NdGaO_3$ substrates to optimize conditions for the growth of high quality single crystal films. X-ray diffraction results show that all the films have one growth direction and well defined peaks in the specular scans with the expected symmetry for each growth orientation. The UO_2/Al_2O_3, TiO_2, and ZnO films have high concentration of misfit dislocations that increase with the lattice mismatch. The UO_2 film on YSZ is found to be in registry with the substrate. The film has narrow mosaic component that is imposed upon a broader component arises from the diffuse scattering due to defects in the film. Meanwhile, $UO_2/NdGaO_3$ film shows a splitting of the X-ray diffraction peaks which is attributed to the in-plane asymmetry of the orthorhombic substrate.

1. Introduction

Uranium dioxide properties have been intensely studied over decades because it the main fuel in nuclear power plants. Most of the studies were performed on bulk and powder samples however there were few attempts to study UO_2 properties in the thin film geometry deposited by various growth methods.

The first known trial to grow thin film of UO_2 was done by Bierlein et al. using vacuum evaporation [1]. They deposited the films on carbon substrate to study radiation damage in nuclear fuel. The evaporation technique was also used in several other studies and for various applications [2–6]; Birjega et al. evaporated polycrystalline UO_2 thin film on three types of NaCl substrates; pure, and doped with Pb or Ag to study the effect of adding impurities to the substrate on the film structure [7]. Shoichi et al. prepared polycrystalline UO_2 thin films on NaCl substrate to study the He ions energy loss in UO_2 [8].

Chemical vapor deposition was used by Shiokawa et al. to grow UO_2 thin films on quartz substrates [9]. They deposited polycrystalline α-U_3O_8, UO_{2+x} ($x > 0.25$), and U_4O_9 at different growth conditions. Amorphous UO_2 was grown from solution on Fe foil by Qiu et al. but several U_4O_9 peaks appeared after annealing [10]. Sol-gel technique was used to deposit films on sapphire and MgO substrates by Meek et al. to study the optical properties of intrinsic and doped UO_2 [11]. Polycrystalline UO_2 thin films were grown at room temperature on Ni substrates using electrodeposition by Adamska et al. [12].

The growth of single crystal UO_2 thin films on a substrate was reported for the first time by Burrell et al. [13] using polymer-assisted chemical solution deposition to grow single crystal UO_2 thin film on $LaAlO_3$ substrate [13,14]. The XRD spectra showed that the film had a strong (100) peak and small (111) peak with intensity <2% relative to the (100) peak.

Sputtering techniques were employed in several studies to grow the thin films. Navinsek used cathode sputtering to grow fine grained polycrystalline and nearly perfect single crystal UO_2 thin films on sodium chloride crystals [15]. Low crystalline UO_2 thin films were deposited on quartz substrate by Miyake et al. [16]. Miserque et al. deposited films on polycrystalline gold disc, single crystal Si, and amorphous glass substrates [17]. Chen et al. succeeded to grow preferentially oriented UO_2 thin films with (111) planes on Si (111) substrate, and also noticed that the crystallinity of the film increased with the thickness [18].

In 2012, we successfully deposited single crystal UO_2 thin films on YSZ and sapphire substrates using reactive gas magnetron sputtering [19]. Our study showed that the change in the oxygen partial pressure can lead to the formation of single crystal UO_2, U_4O_9 and U_3O_8. Following that, we studied the change in the mechanical properties of the thin films under heavy ion irradiation and high temperature and results were similar and relevant to data collected using bulk nuclear fuel samples [20]. This work will open the doors for further research on the usage of thin films as a surrogate for nuclear materials.

* Corresponding author.
E-mail address: elbakhs1@illinois.edu (M.S. Elbakhshwan).

http://dx.doi.org/10.1016/j.tsf.2017.07.020
0040-6090/

The reactive gas magnetron sputtering technique was later adapted in several studies; Bao et al. deposited single crystal UO_2 films on $LaAlO_3$ and CaF_2 substrates to study the magnetic properties [21]. Teterin et al. deposited single crystal and preferentially oriented UO_2 thin films on YSZ and LSAT substrates with different crystallographic orientations [22]. Springell et al. deposited (001), (110) and (111) single crystals UO_2 to study the interfacial interactions between water and spent nuclear fuel [23]. Popel et al. used it to study radiation damage in nuclear fuel [24–27], and finally Cakir et al. used it to study the thorium effect on the oxidation states of UO_2 thin films [28].

The current study shows the ability to grow single crystal UO_2 thin films in various crystallographic orientations by depositing the UO_2 on TiO_2, Al_2O_3, YSZ, ZnO, and $NdGaO_3$ single crystal substrates using the magnetron sputtering technique.

2. Experimental procedure

We deposited Uranium dioxide thin films on different substrates using reactive gas magnetron sputtering [29]. Argon ions were used as a sputtering gas at partial pressure of 8.3×10^{-2} Pa. The sputtering process performed at the current controlling mode, the ion current was fixed during the whole process at 0.056 mA while the power and voltage were around 20 W and 352 V respectively. Before the deposition, the substrates were annealed at 400 °C for two hours followed by another two hours annealing at 750 °C, while the temperature was kept at 700 °C and oxygen partial pressure of 1.3×10^{-5} Pa during the deposition. The substrates were kept rotating at 60 RPM to insure uniform heat distribution and the growth rate was around 6.2 Å/s.

Thin films were deposited simultaneously on five different single crystal substrates which were all oxides to avoid anion diffusion through the film-substrate interface; TiO_2, r-plane Al_2O_3, YSZ (8%moleY_2O_3), ZnO (C-plate), and $NdGaO_3$. All substrates were supplied by MTI Corporation, USA, except Al_2O_3 substrate was supplied by Crystal Gmbh, Germany. Substrates were selected to have different crystal structures and a broad range of lattice parameters as summarized in Table 1.

The film structure and thickness were investigated by X-ray diffraction (XRD) and X-ray reflectivity (XRR) using Philips X'pert machine of Cu K_α radiation of wavelength 1.54056 Å. Fitting of the XRR measurements was performed using the REFLFIT software package from the National Institute of Standards and Technology. Furthermore, Rutherford backscattering (RBS) was done using High Voltage Engineering Van de Graaff accelerator with 2 MeV He^+ ions and the spectrum was fitted using SIMNRA software package [30].

3. Results

The UO_2 thin films were deposited on substrates that have different crystal structure and a broad range of lattice parameters. They have smaller and larger than the lattice parameter of UO_2 (5.47 Å) which has a fluorite crystal structure and space group of Fm3m [31]. The structural and compositional properties of the thin films deposited on each substrate are summarized as follow:

Table 1
Substrate structure and properties.

Substrate	Crystal structure	Orientation
TiO_2 (Rutile)	Tetragonal $a = 4.59$ Å, $c = 2.95$ Å	(100)
Al_2O_3 (*r*-plane)	Hexagonal $a = 4.77$ Å, $c = 13.04$ Å	$(1\bar{1}02)$
YSZ (8% mole Y_2O_3)	Cubic $a = 5.125$ Å	(100)
ZnO (*c*-plate)	Hexagonal $a = 3.25$ Å, $c = 5.31$ Å	(0001) O-face polished
$NdGaO_3$	Orthorhombic $a = 5.43$ Å, $b = 5.50$ Å, $c = 7.7$ Å	(100)

3.1. TiO_2 substrate

The TiO_2 (Rutile) substrate is a single crystal with (100) orientation. It has a tetragonal crystal structure and a space group of p42mnm with lattice parameters of $a = 4.59$ Å and $c = 2.95$ Å [32], as summarized in Table 1. The epitaxial relation between the substrate and the deposited film indicates that the UO_2 lattice is rotated by 26.6° degrees with respect to the surface normal, with d spacing of $(a^2 + c^2)^{1/2} = 5.45$ Å, which fits the UO_2 (100) plane with $a = 5.47$ Å. Therefore, the UO_2 lattice is found to be under compression of −0.3% with respect to the substrate.

XRD shows that the UO_2 thin film deposited on TiO_2 substrate has single (220) growth orientation as shown in Fig. 1. The in-plane ϕ scan shows a broad but well defined peaks with two-fold symmetry for the (110) reflections of the fluorite UO_2 as shown in Fig. 2. The mosaic of the UO_2 film is investigated using the rocking curve scan. The film has a broad mosaic width with FWHM of 5.09, as shown in Fig. 3, indicating that the UO_2 film is not in register with the TiO_2 substrate due to the large difference in the lattice parameters. However the XRD (out-of-plane) and in-plane ϕ scans show that the film is a single crystal. This is an indication that the film has a lot of low-angle tilt boundaries due to the high dislocation density [19].

XRR shows that the film is smooth and uniform with a thickness of 370 Å as shown in Fig. 4. Furthermore, RBS measurement shows that the film-substrate consists of three layers; an oxygen rich layer on the film surface due to air exposure, a stoichiometric UO_2 layer, and finally the substrate. No interdiffusion was observed through the film-substrate interface.

3.2. Al_2O_3 substrate

A single crystal *r*-plane sapphire substrate with $(1\bar{1}02)$ orientation was used for the deposition of UO_2 films. It has a hexagonal crystal structure with a space group of R3c and lattice parameters of $a = 4.77$ Å and $c = 13.04$ Å, as summarized in Table 1.

The deposited film is found to have a single growth orientation of (200) as shown in Fig. 1, with four-fold symmetry in the in-plane ϕ

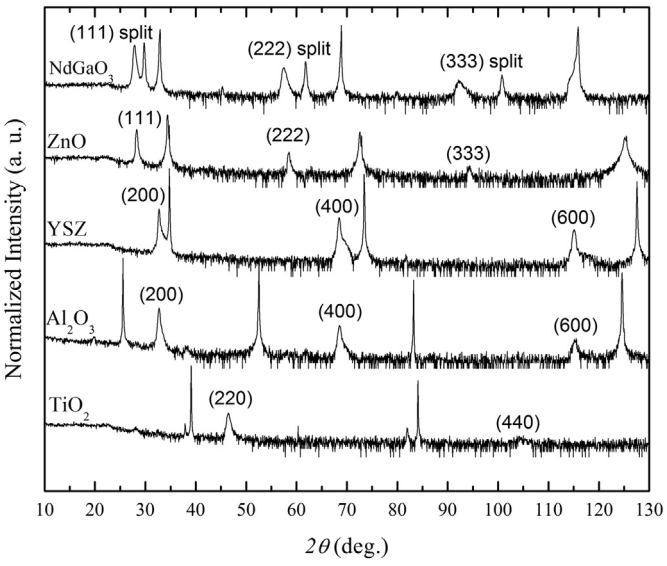

Fig. 1. X-ray diffraction patterns for UO_2 thin films on TiO_2, Al_2O_3, YSZ, ZnO, and $NdGaO_3$ single crystal substrates. The unmarked peaks are for the substrates.

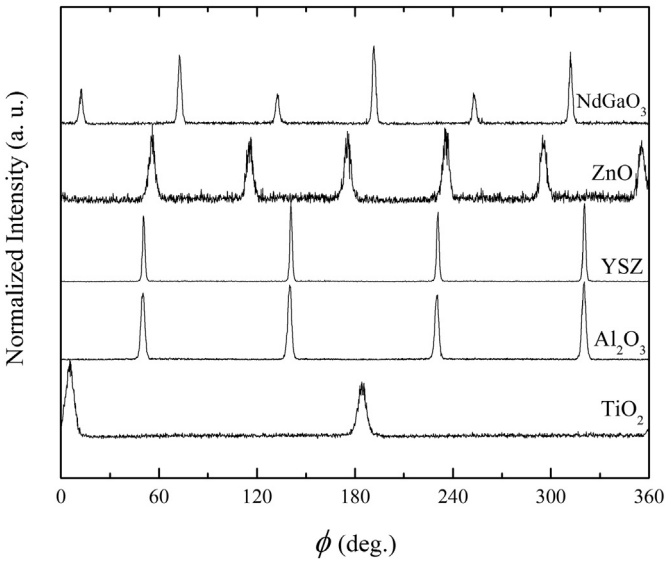

Fig. 2. In-plane ϕ scans for UO_2 thin films deposited on TiO_2, Al_2O_3, YSZ, ZnO, and $NdGaO_3$ single crystal substrates.

scan as shown in Fig. 2. The mosaic broadness is found to improve, versus to the TiO_2 substrate, giving FWHM of 2.34 as shown in Fig. 3. This may indicate that the UO_2 lattice has a better match with Al_2O_3 than TiO_2 but still the film has low-angle tilt boundaries [19]. The film is found to be smooth and uniform as shown in Fig. 4. Finally, RBS shows that the film has an oxygen rich layer on the surface as well as an interdiffusion layer in which the aluminum diffuses into the UO_2 film forming a layer between the stoichiometric UO_2 layer and the substrate. This diffusion occurs mostly because the small atomic size of aluminum which makes it easy to transport through the interface and UO_2 lattice.

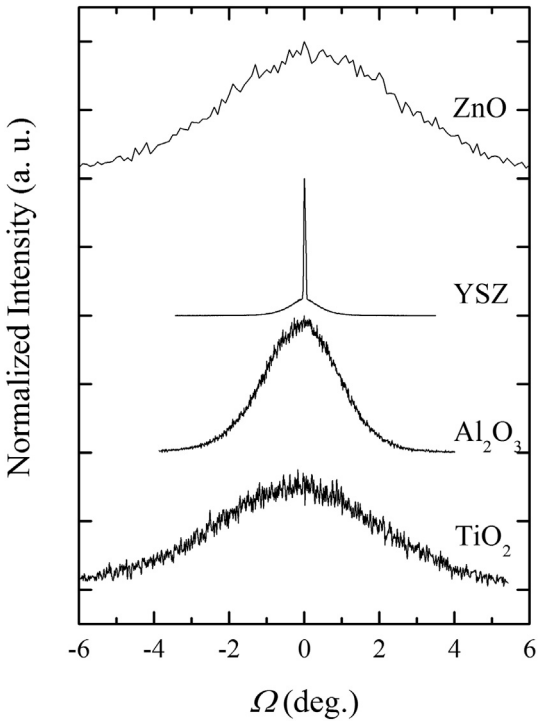

Fig. 3. Rocking curve for UO_2 thin films on TiO_2, Al_2O_3, YSZ, and ZnO single crystal substrates.

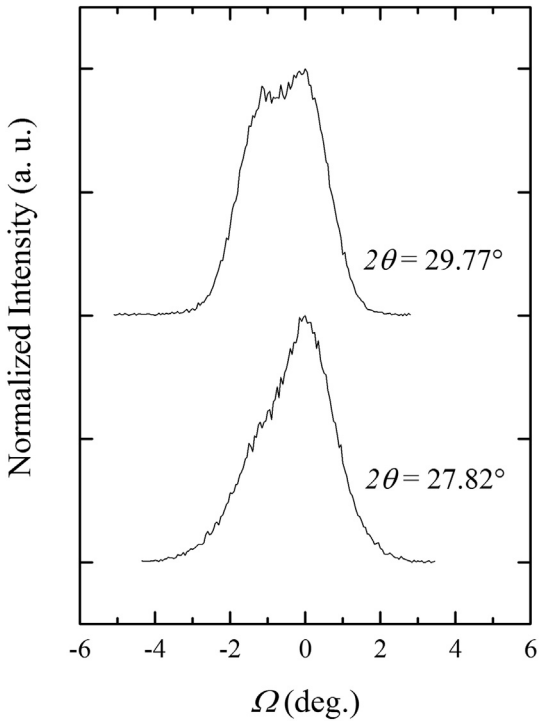

Fig. 4. Rocking curve for UO_2 thin film peak splits on $NdGaO_3$ single crystal substrates.

3.3. YSZ substrate

Yttria-stabilized zirconia (YSZ) is ZrO_2 oxide that is doped by Y_2O_3 to stabilize the cubic phase at room temperatures. In this study YSZ with 8% mole Y_2O_3 is used, it has the same fluorite structure as UO_2 with a lattice parameter of $a = 5.125$ Å. Therefore, the UO_2 film is grown by plane to plane epitaxial matching to the YSZ substrate but with a compression of −6.3% with respect to the substrate. XRD shows that UO_2 film with single growth orientation (200) is deposited on YSZ with the same orientation as shown in Fig. 1. Fig. 2 shows narrow and well defined peaks in the in-plane ϕ scan with a four-fold symmetry. The rocking curve scan shows two components; the narrow component has a FWHM of 0.05 and is found to be imposed upon a broader component with FWHM of 0.99 as shown in Fig. 3. This mosaic broadness is the least among all the films and indicates that UO_2 film deposited on YSZ has the highest degree of crystallinity. This is due to the matching between the film and substrate crystal structures. Again, XRR shows that the film is smooth and RBS results show no signs of diffusion through the film-substrate interface as shown in Figs. 3 and 4.

3.4. ZnO substrate

A thin film of UO_2 is deposited on a single crystal of *c*-plate ZnO substrate with (0001) orientation. It has a hexagonal crystal structure with lattice parameters of $a = 3.25$ Å and $c = 5.31$ Å as summarized in Table 1.

After deposition, UO_2 film has a single growth orientation of (111) as shown in Fig. 1, and the film has a six-fold symmetry with broad peaks in the in-plane ϕ scan as shown in Fig. 2. The film has the highest mosaic broadness with FWHM of 5.64, indicating that it has the highest dislocation density and so the least crystalline quality as shown in Fig. 3. In addition, the film has a rough surface as observed by the XRR scans in Fig. 4. No interdiffusion is observed between the film and the substrate as shown in Fig. 5.

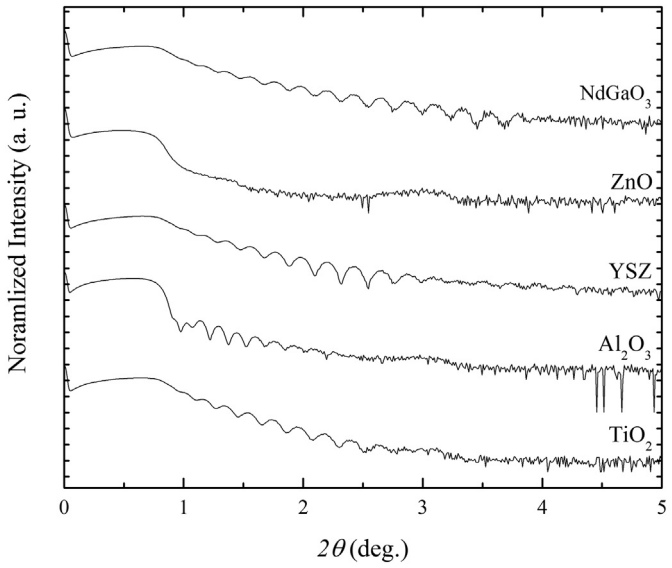

Fig. 5. X-ray reflectivity scans for UO_2 thin films deposited on TiO_2, Al_2O_3, YSZ, ZnO, and $NdGaO_3$ single crystal substrates.

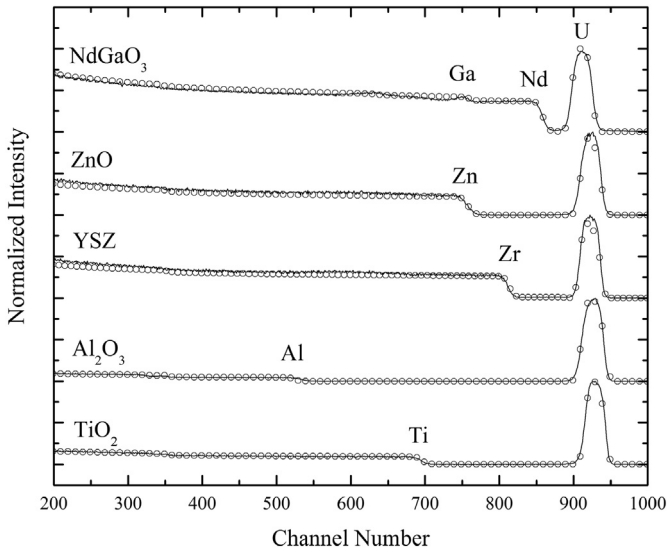

Fig. 6. RBS measurements for UO_2 thin films deposited on TiO_2, Al_2O_3, YSZ, ZnO, and $NdGaO_3$ single crystal substrates. The solid line represents the experimental data while the circles represent the best fitting. The elemental peaks are identified in the figure.

3.5. $NdGaO_3$ substrate

The final substrate used in the study is a single crystal $NdGaO_3$ with (100) orientation. It has an orthorhombic crystal structure with lattice parameters of $a = 5.43$ Å, $b = 5.50$ Å, and $c = 7.7$ Å as summarized in Table 1. The crystal structure of the deposited UO_2 film shows a very interesting phenomenon; it has a (111) growth orientation similar to the film deposited on ZnO substrate, but each diffraction peak split into two components located at both sides of the expected peak position for the (111) reflection as shown in Fig. 1. Furthermore, the in-plane ϕ scan shows that the film has a six-fold symmetry but the peaks are divided into two groups with different peak intensities as shown in Fig. 2. This indicates that the film experiences compressive and tensile stresses simultaneously.

This behavior has not been noticed with the other substrates because all of them have the lattice parameters a and b are less than that of UO_2. Therefore the UO_2 lattice always experiences a single type of stress (compression stress) with respect to the substrate. The $NdGaO_3$ substrate is the only substrate that has an orthorhombic structure in which $a_{substrate} \neq b_{substrate}$ and $a_{substrate} < a_{film} < b_{substrate}$. This may explain why the film experiences both compression and tension stresses simultaneously and so the split of the XRD peaks. The rocking curve scans show that the peak splits are not uniform and have different mosaic broadness with FWHM of 2.35 and 2.43 for components at diffraction angle 2θ of 27.82° and 29.79° respectively as shown in Fig. 6. RBS measurements are similar to the other films with no interdiffusion. The only difference noticed is the shifting of the UO_2 peak toward lower energy values. This is attributed to the high atomic number elements in the substrate (Nd and Ga) which increase the scattering probability (the scattering probability is proportional to the square of the atomic number of the target material) [33], therefore, the backscattered particles have less energy compared to the other samples.

4. Discussion

The growth of single crystal UO_2 thin films using magnetron sputtering is performed on five different substrates. In order to claim that thin film has a single crystal structure, the film should have: (1) single growth orientation in the specular scans normal to the film-substrate interface, (2) fold symmetry consistent with the growth domain, and (3) narrow mosaic of the crystallographic reflections [19]. Films deposited on TiO_2, Al_2O_3, and ZnO substrates are found to clearly satisfy the first two conditions as shown in Figs. 1 and 2, but they have a broad mosaic as summarized in Table 2. This mosaic broadness does not imply that the films are polycrystals or textured, but they contain high concentrations of low-angle tilt boundaries due to the high dislocation density.

For the films deposited on hexagonal substrates ZnO and Al_2O_3, the FWHM is found to increase with the difference in lattice parameters. Therefore, results show that UO_2/ZnO has boarder mosaic than UO_2/Al_2O_3 as well as it has the lowest epitaxial quality of all films due to the huge difference in lattice parameters compared to UO_2. When films deposited on substrates with lattice parameter mismatch, the film strained till a certain thickness (the critical thickness), after which the film releases some of the strain energy by forming misfit dislocations [34–36]. The concentration of those dislocations increases with the lattice mismatch between the film and the substrate [37–39].

On the other hand, the YSZ substrate has a closer lattice parameter to UO_2 as well as the same crystal structure, and so the film is in registry with the substrate. The film not only has a single growth orientation and the associated symmetry, but also has the least mosaic broadness among all substrates. In our previous work, we showed that this behavior is maintained up to thicknesses of 856 Å [19]. This indicates that UO_2/YSZ has the highest quality film comparing to all other substrates. Similar conclusion was obtained by Bao et al. when they deposited UO_2 on hexagonal $LaAlO_3$ and cubic CaF_2. UO_2/CaF_2 was found to have much higher quality than UO_2/$LaAlO_3$ because it has a very close lattice parameter and the same crystal structure to UO_2 [21]. The two components in the rocking curve of UO_2/YSZ were observed in various thin films systems [40–44]. The broad component arises from the diffuse scattering due to distorted regions in the crystal around defects such as dislocations and grain boundaries, while the narrow component is attributed to the long range order of the coherent part of the crystal structure [40,41].

Table 2
UO_2 film orientation, lattice parameter, and FWHM on five different substrates.

Substrate	Film orientation	Film lattice parameter (Å)	FWHM
TiO_2	(220)	5.51	5.09
Al_2O_3	(200)	5.46	2.34
YSZ[a]	(2 0 0)	5.48	0.05/0.99
ZnO	(111)	5.47	5.64
$NdGaO_3$[b]	(1 1 1) with split	5.54/5.19	2.35/2.43

[a] FWHM for both narrow and broad components respectively.
[b] Lattice parameters and FWHM for the two peak splits of the (111) orientation.

The deposition on the orthorhombic $NdGaO_3$ substrate is found to be unique. The film experiences a splitting of the (111) growth reflections, with a broad and asymmetric mosaic as shown in Figs. 1 and 3. In addition, the in-plane ϕ scan shows that the film has two different domains. This behavior is attributed to the in-plane asymmetry of the $NdGaO_3$ substrate ($a_{substrate} \neq b_{substrate}$ and $a_{substrate} < a_{film} < b_{substrate}$) [45], which creates different stress levels on the film lattice and leads to the splitting of the diffraction peaks. These results are known for different types of films deposited on orthorhombic substrates. For instances; two stripe domains were observed in epitaxial (001) $BiFeO_3$ thin films on the orthorhombic $TbScO_3$ substrate [46]. Chen et al. noticed a splitting in the diffraction peaks of $BiFeO_3$ epitaxial thin films on $PrScO_3$ orthorhombic substrate and attributed that to the presence of two tilted domains in the films [47]. Duk et al. found that two domains formed in thick $NaNbO_3$ thin films deposited on (110) $TbScO_3$ orthorhombic substrate [48].

Meanwhile, it is worth mentioning that we only measured the out-of-plane lattice parameters for all the films. However additional measurements of the in-plane lattice parameters would allow understanding how the lattice mismatch and associated strain levels in the film could distort the film lattice.

In conclusion, the UO_2 thin films grown on TiO_2, Al_2O_3, YSZ, ZnO, and $NdGaO_3$ substrates are all single crystals. These results show that UO_2 can be deposited in several crystallographic orientations and under different stress domains which can provide more understanding of the nuclear fuel behavior in highly controlled conditions and environments. It also provides those advantages with minor amounts of radioactivity and toxicity, which makes the nuclear fuel research and development more accessible [14,49–51].

5. Summary

Single crystal UO_2 thin films are deposited on TiO_2, Al_2O_3, YSZ, ZnO, and $NdGaO_3$ substrates. All the films have single growth orientation but the film deposited on $NdGaO_3$ shows a splitting in the (111) reflections peaks due to the in-plane asymmetry of the substrate. Film deposited on the YSZ substrate has the least mosaic broadness. RBS results show that the surface layer of each film is hyperstoichiometric due to the air exposure and the aluminum diffuses into the UO_2 film under those growth conditions.

Acknowledgements

This work was performed with support from the US Department of Energy Nuclear Research Initiative under Grant No. DEFG-07-14891. In addition, this work was carried out in part in the Frederick Seitz Materials Research Laboratory Central Facilities, University of Illinois, which are partially supported by the US Department of Energy under Grants DE-FG02-07ER46453 and DE-FG02-07ER46471.

References

[1] T. Bierlein, B. Mastel, Damage in UO2 films and particles during reactor irradiation, J. Appl. Phys. 31 (1960) 2314.
[2] F. Vasiliu, V. Topa, N. Pogrion, M. Birjega, Electronmicroscopical studies of UO2 thin films evaporated on NaCl substrates with colloidal centres, Jpn. J. Appl. Phys. 13 (1974) 605–607.
[3] S. Steeb, Elektronenbeugungs-untersuchung an einkristallinen schichten von uranoxyden im bereich von UO2 bis U4O9, J. Nucl. Mater. 3 (1961) 235–236.
[4] S. Steeb, P. Mitsch, bestimmung der zwischengitterverteilung von sauerstoffatomen mittels elektronenbeugung an einkristallinen urandioxydschichten, J. Nucl. Mater. 15 (1965) 81–87.
[5] E. Horl, P. Heilmann, Epitaxial growth of UO2 on graphite, J. Nucl. Mater. 21 (1967) 96.
[6] N. Pggrion, F. Vasiliu, M. Bîrjega, The structure of vacuum-evaporated UO2 thin films, J. Nucl. Mater. 51 (1974) 255–260.
[7] M. Bîrjega, N. Pogrion, V. Topa, F. Vasiliu, Epitaxial growth of UO2 thin films evaporated on NaCl substrates with colloidal centres, J. Nucl. Mater. 51 (2) (1974) 261–265.
[8] S. Nasu, K. Ozawa, K. Shiozawa, K. Kawatsura, T. Kurasawa, He+ ion energy loss parameter in thin films of UO2, J. Nucl. Mater. 73 (2) (1978) 213–216.
[9] Y. Shiokawa, R. Amano, A. Nomura, M. Yagi, Preparation of lanthanide, thorium and uranium oxide films by chemical vapor deposition using β-diketone chelates, J. Radioanal. Nucl. Chem. 152 (2) (1991) 373–380.
[10] S. Qiu, C. Amrhein, M. Hunt, R. Pfeffer, B. Yakshinskiy, L. Zhang, T. Madey, J. Yarmoff, Characterization of uranium oxide thin films grown from solution onto Fe surfaces, Appl. Surf. Sci. 181 (3–4) (2001) 211–224.
[11] T. Meek, B. Roedern, P. Clem, R. Hanrahan Jr., Some optical properties of intrinsic and doped UO2 thin films, Mater. Lett. 59 (2005) 1085–1088.
[12] A. Adamska, E. Bright, J. Sutcliffe, W. Liu, O. Payton, L. Picco, T. Scott, Characterisation of electrodeposited polycrystalline uranium dioxide thin films on nickel foil for industrial applications, Thin Solid Films 597 (2015) 57–64.
[13] A. Burrell, T. McCleskey, P. Shukla, H. Wang, T. Durakiewicz, D. Moore, C. Olson, J. Joyce, Q. Jia, Controlling oxidation states in uranium oxides through epitaxial stabilization, Adv. Mater. 19 (21) (2007) 3559–3563.
[14] B. Scott, J. Joyce, T. Durakiewicz, R. Martin, T. McCleskey, E. Bauer, H. Luo, Q. Jia, High quality epitaxial thin films of actinide oxides, carbides, and nitrides: advancing understanding of electronic structure of f-element materials, Coord. Chem. Rev. 266-267 (2014) 137–154.
[15] B. Navinsek, Epitaxial growth of UO2 thin films produced by cathode sputtering, J. Nucl. Mater. 40 (1971) 338–340.
[16] C. Miyake, Y. Yoneda, M. Matsumura, T. Iida, K. Taniguchi, T. Yamanaka, M. Yamanaka, T. Yamamoto, Characterization of uranium oxide thin film prepared by vacuum deposition method, J. Nucl. Sci. Technol. 27 (4) (1990) 382–385.
[17] F. Miserque, T. Gouder, D. Wegen, P. Bottomley, Use of UO2 films for electrochemical studies, J. Nucl. Mater. 298 (3) (2001) 280–290.
[18] Q. Chen, X. Lai, B. Bai, M. Chu, Structural characterization and optical properties of UO2 thin films by magnetron sputtering, Appl. Surf. Sci. 256 (10) (2010) 3047–3050.
[19] M. Strehle, B. Heuser, M. Elbakhshwan, X. Han, D. Gennardo, H. Pappas, H. Ju, Characterization of single crystal uranium-oxide thin films grown via reactive-gas magnetron sputtering on yttria-stabilized zirconia and sapphire, Thin Solid Films 520 (17) (2012) 5616–5626.
[20] M. Elbakhshwan, Y. Miao, J. Stubbins, B. Heuser, Mechanical properties of UO2 thin films under heavy ion irradiation using nanoindentation and finite element modeling, J. Nucl. Mater. 479 (2016) 548–558.
[21] Z. Bao, R. Springell, H. Walker, H. Leiste, K. Kuebel, R. Prang, G. Nisbet, S. Langridge, R. Ward, T. Gouder, R. Caciuffo, G. Lander, Antiferromagnetism in UO2 thin epitaxial films, Phys. Rev. B 88 (2013) 134426.
[22] Y. Teterin, A. Popel, K. Maslakov, A. Teterin, K. Ivanov, S. Kalmykov, R. Springell, T. Scott, I. Farnan, XPS study of ion irradiated and unirradiated UO2 thin films, Inorg. Chem. 55 (16) (2016) 8059–8070.
[23] R. Springell, S. Rennie, L. Costelle, J. Darnbrough, C. Stitt, E. Cocklin, C. Lucas, R. Burrows, H. Sims, D. Wermeille, J. Rawle, C. Nicklin, Water corrosion of spent nuclear fuel: radiolysis driven dissolution at the UO2/water interface, Faraday Discuss. 180 (2015) 301–311.
[24] A. Popel, V. Petrov, V. Lebedev, J. Day, S. Kalmykov, R. Springell, T. Scott, I. Farnan, The effect of fission-energy Xe ion irradiation on dissolution of UO2 thin films, J. Alloys Compd. 721 (2017) 586–592.
[25] A. Popel, A. Adamska, P. Martin, O. Payton, G. Lampronti, L. Picco, L. Payne, R. Springell, T. Scott, I. Monnet, C. Grygiel, I. Farnan, Structural effects in UO2 thin films irradiated with U ions, Nucl. Instrum. Methods Phys. Res., Sect. B 386 (2016) 8–15.
[26] A. Popel, V. Lebedev, P. Martin, A. Shiryaev, G. Lampronti, R. Springell, S. Kalmykov, T. Scott, I. Monnet, C. Grygiel, I. Farnan, Structural effects in UO2 thin films irradiated with fission-energy Xe ions, J. Nucl. Mater. 482 (2016) 210–217.
[27] A. Popel, S. Solliec, G. Lampronti, J. Day, P. Petrov, I. Farnan, The effect of fission-energy Xe ion irradiation on the structural integrity and dissolution of the CeO2 matrix, J. Nucl. Mater. 484 (2017) 332–338.
[28] P. Cakir, R. Eloirdi, F. Huber, R. Konings, T. Gouder, Thorium effect on the oxidation of uranium: photoelectron spectroscopy (XPS/UPS) and cyclic voltammetry (CV) investigation on (U1 − xThx)O2 (x = 0 to 1) thin films, Appl. Surf. Sci. 393 (2017) 204–211.
[29] S. Berg, T. Nyberg, Fundamental understanding and modeling of reactive sputtering processes, Thin Solid Films 476 (2005) 215–230.
[30] SIMNRA Version 6.06. Max-Planck-Institut für Plasmaphysik, (Germany).
[31] H. Idriss, Surface reactions of uranium oxide powder, thin films and single crystals, Surf. Sci. Rep. 65 (3) (2010) 67–109.
[32] A. Lotnyk, S. Senz, D. Hesse, Epitaxial growth of TiO2 thin films on SrTiO3, LaAlO3 and yttria-stabilized zirconia substrates by electron beam evaporation, Thin Solid Films 515 (2007) 3439–3447.
[33] W. Mayer, E. Rimini, Ion Beam Handbook for Material Analysis, Academic Press, 1977.
[34] M. Choudhary, J. Kundin, Heteroepitaxial anisotropic film growth of various orientations, J. Mech. Phys. Solids 101 (2017) 118–132.
[35] E. Grier, M. Jenkins, A. Petford-Long, R. Ward, M. Wells, Misfit dislocations of epitaxial (110) niobiumi ‖ (1120) sapphire interfaces grown by molecular beam epitaxy, Thin Solid Films 358 (2000) 94–98.
[36] H. Hattab, G. Jnawali, M. Hoegen, In-situ high-resolution low energy electron diffraction study of strain relaxation in heteroepitaxy of Bi(111) on Si(001): Interplay of strain state, misfit dislocation array and lattice parameter, Thin Solid Films 570 (2014) 159–163.
[37] Y. Sidorov, M. Yakushev, A. Kolesnikov, Dislocations in CdTe heteroepitaxial structures on GaAs(301) and Si(301) substrates, Optoelectronics, Instrumentation and Data Processing 50 (3) (2014) 234–240.

[38] Frédéric Bonell, Stéphane Andrieu, Electron diffraction study of the plastic relaxation of MgO epitaxially grown on BCC FeV(001) alloys by varying the lattice mismatch, Surf. Sci. 656 (2017) 140–147.
[39] J. Du, Y. Fang, E. Fu, X. Ding, K. Yu, Y. Wang, Y. Wang, J. Baldwin, P. Wang, Q. Bai, What determines the interfacial configuration of Nb/Al2O3 and Nb/MgO interface, Sci Rep 6 (2016) 33931.
[40] C. Hubault, C. Davoisne, A. Boulle, L. Dupont, V. Demange, A. Perrin, B. Gautier, J. Holc, M. Kosec, M. Karkut, N. Lemee, Strain effect in PbTiO3/PbZr0.2Ti0.8O3 superlattices: from polydomain to monodomain structures, J. Appl. Phys. 112 (2012) 114102.
[41] O. Durand, A. Letoublon, D. Rogers, F. Teherani, Interpretation of the two-components observed in high resolution X-ray diffraction ω scan peaks for mosaic ZnO thin films grown on c-sapphire substrates using pulsed laser deposition, Thin Solid Films 519 (2011) 6369–6373.
[42] P. Fewster, X-ray diffraction from low-dimensional structures, Semicond. Sci. Technol. 8 (1993) 1915–1934.
[43] P. Fewster, X-ray analysis of thin films and multilayers, Rep. Prog. Phys. 59 (1996) 1339–1407.
[44] P. Kidd, P. Fewster, N. Andrew, Interpretation of the diffraction profile resulting from strain relaxation in epilayers, J. Phys. D. Appl. Phys. 28 (1995) A133–A138.
[45] S. Chae, Y. Chang, S. Seo, T. Noh, D. Kim, C. Jung, Epitaxial growth and the magnetic properties of orthorhombic YTiO3 thin films, Appl. Phys. Lett. 89 (2006) 182512.
[46] C. Folkman, S. Baek, H. Jang, C. Eom, C. Nelson, X. Pan, Y. Li, L. Chen, A. Kumar, V. Gopalan, S. Streiffer, Stripe domain structure in epitaxial (001) BiFeO3 thin films on orthorhombic TbScO3 substrate, Appl. Phys. Lett. 94 (2009) 251911.
[47] Z. Chen, Y. Qi, L. You, P. Yang, C. Huang, J. Wang, T. Sritharan, L. Chen, Large tensile-strain-induced monoclinic MB phase in BiFeO3 epitaxial thin films on a PrScO3 substrate, Phys. Rev. B 88 (2013), 054114.
[48] A. Duk, M. Schmidbauer, J. Schwarzkopf, Anisotropic one-dimensional domain pattern in NaNbO3 epitaxial thin films grown on (110) TbScO3, Appl. Phys. Lett. 102 (2013), 091903.
[49] A. Adamska, R. Springell, A. Warren, L. Picco, O. Payton, T. Scott, Growth and characterization of uranium-zirconium alloy thin films for nuclear industry applications, J. Phys. D. Appl. Phys. 47 (2014) 315301.
[50] A. Adamska, R. Springell, T. Scott, Characterization of poly- and single-crystal uranium-molybdenum alloy thin films, Thin Solid Films 550 (2014) 319–325.
[51] J. Nelson, Uranium: Sources, Nova Science Publishers, Exposure and Environmental Effects, 2015.